Hindawi
Complexity
Volume 2020, Article ID 4134851, 13 pages
https://doi.org/10.1155/2020/4134851

Research Article

Optimizing Transmit Sequence and Instrumental Variables Receiver for Dual-Function Complexity System

Yu Yao,[1] **Junhui Zhao**,[1] **and Lenan Wu**[2]

[1]*East China Jiaotong University, Nanchang, China*
[2]*Southeast University Nanjing, Nanchang, China*

Correspondence should be addressed to Yu Yao; 1057604987@qq.com

Received 9 August 2019; Accepted 30 December 2019; Published 20 January 2020

Guest Editor: Francisco G. Montoya

This correspondence deals with the joint cognitive design of transmit coded sequences and instrumental variables (IV) receive filter to enhance the performance of a dual-function radar-communication (DFRC) system in the presence of clutter disturbance. The IV receiver can reject clutter more efficiently than the match filter. The signal-to-clutter-and-noise ratio (SCNR) of the IV filter output is viewed as the performance index of the complexity system. We focus on phase only sequences, sharing both a continuous and a discrete phase code and develop optimization algorithms to achieve reasonable pairs of transmit coded sequences and IV receiver that fine approximate the behavior of the optimum SCNR. All iterations involve the solution of NP-hard quadratic fractional problems. The relaxation plus randomization technique is used to find an approximate solution. The complexity, corresponding to the operation of the proposed algorithms, depends on the number of acceptable iterations along with on and the complexity involved in all iterations. Simulation results are offered to evaluate the performance generated by the proposed scheme.

1. Introduction

Radar and wireless communication systems have always been researched independently. On the one hand, the radar system attempts to gain better target detection performance in the presence of noise interference. On the other hand, the aim of the wireless communication technique is to achieve the maximum information capacity over a noisy channel [1–3]. The works of [4–9] showed a possibility of employing the radar-communications integration concept to solve the lack of radio frequency (RF) spectrum. Efficient utilization of shared bandwidth between wireless communications and radar can be achieved by using dynamic frequency allocation. Ahmed at al. presented a joint radar-communication scheme to embed quadrature amplitude modulation-(QAM-) based communication data in the radar pulses. In [10, 11], the authors developed a dual-function complexity system capable of performing radar and communication tasks. The complexity system performs both tasks by optimizing the power allocation of the diverse transmitters. The proposed technique serves manifold communication receivers positioned in the vicinity of the complexity system. Numerous recent studies [12–14] considered that the developing concept of DFRC is secondary as the main radar task. Communication source embedding into the illumination of the radar system is realized using waveform diversity, sidelobe control, or time modulated array technique, which was studied in [13]. Hassanien et al. presented a signaling strategy for communication source embedding into the illumination of an FH-based MIMO radar system [15]. The main principle behind the signaling strategy is to embed phase modulation (PM)-based symbols by using phase rotating the FH pulses. The phase shift is implemented to each transmit FH pulse waveform of the radar system. The PM-based symbol embedding does not influence the function of the radar system, which uses the FH waveforms.

The performance of a radar system is prominently enhanced by sensibly optimizing receive filter and transmitted waveform. This optimization strategy generally copes with some problems containing the existence of signal-dependent

clutter along with signal-independent noise at the receiving end and radar signal constraint, such as similarity to a particular coded sequence. For a nonextended target hidden in the clutter interference environment, joint design of the transmission waveform and radar receiver to optimizing the signal-to-interference-and-noise ratio (SINR) were studied, considering a transmit power and a similarity constraints [16] on the transmission signal. The work of [17] developed a novel cognitive design method for the joint optimization of the phase-modulated (PM) pulse sequence and receive filter, representing a similarity between transmit waveform and a prearranged coded sequence. In [18], the authors developed novel approaches for maximizing the mean-square error of target feature estimation in the presence of clutter interference. For a nonmoving object, in [19], the authors used a frequency domain method to find an optimum energy spectral density (ESD) of the transmitted waveform and corresponding suitable receive filter and presented a synthesis technique to offer the time domain waveform. In [20], the authors considered a joint design problem to that of [19] subject to peak-to-average power ratio (PAR) and transmit power constraint. The work of [21] dealt with the joint design of constant-modulus transmit waveform and receive filter under a transmit power constraint. Some studies considered the joint optimization problem in signal-dependent and signal-independent disturbance scenarios (see, for example, [22–26]). In [24, 26], for a moving object, the unknown Doppler shift has been considered in the transmit waveform design. De Maio et al. discussed the problem of Doppler robust waveform optimization for signal-independent disturbance environment under similarity and transmit power constraint. In a signal-dependent interference environment, the work of [24] was generalized in [26] where the PAR and transmit power constraints are forced as well.

The usage of a matched filter can be considered as an ideal choice only when signal-dependent disturbance does not exist in the radar environment. The abovementioned problem can be tackled by utilizing an instrumental variables (IV) filter instead of the matched filter. The usage of the IV receive filter estimates in pulse compression radar has been distinctly presented many years ago(see, for example, [27, 28] and the references therein). The IV receiver can reject clutter more efficiently than the match filter. Furthermore, the radar waveform design related with the IV receive technique is a motivating research direction.

In this paper, we discuss the joint design problem of the probing coded sequence and IV filter for a DFRC system in the presence of signal-dependent interference, focusing on either continuous or discrete phase codes. Different from a transmit power constraint, we impose a similarity constraint to regulate several characteristics of the transmit waveform, for instance, variations in the waveform modulus and peak sidelobe level. The SCNR is considered as figure of merit. Thus, we present a reasonable coded sequence and IV receive filter, under a similarity constraint between the wanted coded sequence and a given waveform [29–31].

We develop constrained optimization techniques that consecutively enhance the SCNR. All iterations involve the solution of NP-hard quadratic fractional problems. The relaxation plus randomization technique [30] is used to find an approximate solution. The complexity, corresponding to the operation of the proposed algorithms, depends on the number of acceptable iterations along with on and the complexity involved in all iterations. The performance of the proposed scheme is evaluated in signal-dependent interference surroundings, presenting that remarkable SCNR enhancements are achieved jointly designing the transmitted coded sequences and IV receive filter.

The organization of this paper is as follows. In Section 2, we describe the dual-function complexity system and the PM-based FH signal model. In Section 3, we introduce an IV filter for sensing receiver design. In Section 4, we formulate the constrained optimization problems for the joint design of the transmitted coded sequence and the IV filter. Moreover, we develop two successive optimization processes to produce a suitable coded sequence and IV receive filter to these problems. The simulation results demonstrating the proposed algorithms are presented in Section 5. Finally, our conclusions and directions for possible future work are drawn in Section 6.

1.1. Notation. Throughout this paper, the following notations will be used. We use boldface lowercase letters and boldface uppercase letters to denote vectors $\mathbf{c}$ and matrices $\mathbf{C}$, respectively. The ith element of $\mathbf{c}$ and the (i, k)th entry of $\mathbf{C}$ are denoted by c_i and $\mathbf{C}_{ik}$, respectively. We use $(.)^*$ to denote the conjugate operation, $(.)^T$ to denote the transpose operation, $(.)^H$ to denote the Hermitian operation, $E[\cdot]$ to denote statistical expectation, $\mathrm{tr}(\cdot)$ to denote the trace of the square matrix argument, and $\mathbf{0}$ and $\mathbf{I}$ to indicate the matrix with zero entries and the identity matrix, respectively. $\mathbf{A} \geq \mathbf{B}$ means that $\mathbf{A} - \mathbf{B}$ is an Hermitian positive semidefinite matrix. The set of real and complex numbers is denoted by $\mathbb{R}$ and $\mathbb{C}$, respectively. The real parts of x is denoted by $\Re(x)$. The argument and the modulus of x are denoted by $\arg(x)$ and $|x|$, respectively. $\|\mathbf{x}\|$ is the Euclidean norm of the vector $\mathbf{x}$. $\|\mathbf{x}\|_\infty = \max_{k\in(1,\ldots,N)}|x(k)|$ is the l_∞ norm of the vector $\mathbf{x}$. $|.|$ denotes the determinant of a matrix. Finally, the letter $j = \sqrt{-1}$ indicates the imaginary unit.

2. Dual-Function System Configuration

We introduce the configuration for the DFRC system and the PM-based FH signal model [14]. The signal model is the special case of the quadrature amplitude modulation-(QAM-) based approach [6]. The key objective of the dual-function transmitter is to embed communication source toward the direction(s) of the communication receiver(s) as a subordinate mission without disturbing the primary mission, i.e., the radar function. We denote the FH waveform during one radar pulse as

$$\phi(t) = \sum_{q=1}^{Q} e^{j2\pi c_q \Delta f t} u(t - \Delta t). \tag{1}$$

In (1), $c_q, q = 1, \ldots, Q$ describes the FH code and Q denotes the length of the FH code. Δf and Δt are the frequency

step and the hopping interval duration, respectively, and $u(t) = \begin{cases} 1, & 0 < t < \Delta t \\ 0, & \text{otherwise} \end{cases}$. Notice that the FH code can also be written as the multicarrier model [32]. The duration of a radar pulse can be given by $T_0 = Q\Delta t$. Consider that the FH code $c_q \in \{1, ..., J\}$, where J describes a predefined value. Next, we discuss the PM-based information embedding strategy. Let $\{\Omega_q \in [0, 2\pi]\}, q = 1, ..., Q$ be a set of Q phase symbols. Then, PM-based FH waveform can be defined as

$$s(t) = \sum_{q=1}^{Q} e^{j\Omega_q} e^{j2\pi c_q \Delta f t} u(t - \Delta t). \tag{2}$$

During a certain radar pulse, the PM-based FH transmit waveform is shown in Figure 1.

We consider that a phase symbol signifies B bits of binary sequence. During the ith radar pulse, the binary communication information that desires to be embedded is utilized to choose phase symbols $\Omega_q(i), q = 1, ..., Q$ from a preassigned constellation of $K = 2^B$ symbols. We consider the constellation is uniformly distributed between 0 and 2π, which can be expressed by $\mathbb{C}_{\text{PSK}} = \{0, (2\pi/K), ..., ((K-1)\ 2\pi/K)\}$. The PM-based FH waveform can be rewritten as

$$s(t, i) = \sum_{q=1}^{Q} e^{j\Omega_q(i)} e^{j2\pi c_q \Delta f t} u(t - \Delta t). \tag{3}$$

The term $\Omega_q(i) \in \mathbb{C}_{\text{PSK}}$. To simplify the discussion, we consider that a communication receiver is located at a known direction θ_c. Therefore, the received signal at the output of the communication receiver is expressed as

$$y(t, i) = \alpha_c s(t, i) + n(t, i), \tag{4}$$

where α_c describes the propagation channel coefficient. We assume that the coefficient α_c remain unchanged during the whole processing interval. $n(t, i)$ is the zero-mean white Gaussian noise with covariance δ_w^2. At the communication receiver, it has full knowledge of the FH code c_q and the FH step Δf. Notice that we assume the communication receiver is the privacy breach for the radar system. Hassanien et al. stated similar assumption as well. Therefore, the received signals observed at the output of the communication receiver are match-filtered to the FH waveform yielding

$$\begin{aligned} r_q(i) &= \int_0^{\Delta t} y(t, i) e^{-j2\pi c_q \Delta f t} u(t - \Delta t) \mathrm{d}t, \\ &= \alpha_c e^{-j\pi \sin\theta_c} e^{\Omega_q(i)} + n_q(i). \end{aligned} \tag{5}$$

This implies that the communication receiver has the ability to undo $e^{-j\pi \sin\theta_c}$ before it estimates the symbol $\Omega_q(i)$. As a result, the embedded symbol $\Omega_q(i)$ can be restored from $r_q(i)$ at the output of the matched filter. It facilitates the receiver to update its direction with respect to the dual-function transmitter as well. The phase symbols that desire to be embedded can be estimated as

$$\widehat{\Omega}_q(i) = \text{Angle}\big(r_q(i)\big) - \text{Angle}\big(\alpha_c\big) + 2\pi \sin\theta_c. \tag{6}$$

Once the phase shift keying (PSK) symbol has been estimated, then the receiver compares the estimates to the preassigned constellation $\mathbb{C}_{\text{PSK}}$. It allows the receiver to determine the PM-based symbols and convert the symbols into the original binary data. Several papers proposed the PM-based DFRC system and corresponding waveform design approach (see [13] and references therein).

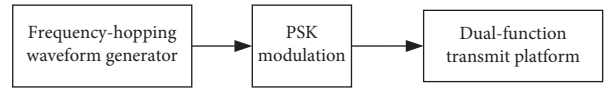

Figure 1: Illustrative diagram of a dual-function transmitter using FH waveform and PSK modulation.

Since target detection is the main task of the proposed DFRC system, transmit waveform should be considered primarily based on the requirements of the radar function. Let $\mathbf{s} = [s(0), s(1), ..., s(N-1)]^T \in \mathbb{C}^N$ be the FH-coded sequences. Let α_0 be a factor that is relative to the radar cross section (RCS) of the range bin of interest irradiated by the proposed DFRC system. Let $\{\alpha_i\}_{i=-N+1, n\neq 0}^{N-1}$ be the factors for the adjacent range bins or clutter patches. Notice that targets might exist at the adjacent range bins. $\forall i \in \{-(N-1), ..., N-1\}$. $\mathbf{J}_i$ denotes the $N \times N$ "shift" matrix that takes into account the fact that the clutter returning from adjacent range bins need different propagation times to reach the DFRC system receiver:

$$\mathbf{J}_i(l, m) = \begin{cases} 1, & \text{if } m - l = n \\ 0, & \text{if } m - l \neq n \end{cases}, \quad (l, m) \in \{1, ..., N\}^2. \tag{7}$$

The target scattering signals that arrive at the receiving end of the proposed DFRC system are demodulated and analog-to-digital converted. Then, the received FH coded sequences can be denoted as

$$\mathbf{y} = \alpha_0 \mathbf{s} + \sum_{i=-N+1, n\neq 0}^{N-1} \alpha_i \mathbf{J}_i \mathbf{s} + \mathbf{n}, \tag{8}$$

where $\mathbf{y} = [y(0), y(1), ..., y(N-1)]^T \in \mathbb{C}^N$. To simplify the analysis, we consider perfect synchronization between diverse dual-function complexity systems. The dual-function radar-communication operation is shown in Figure 2.

3. IV Receive Filter

The technique of IV can be utilized in sensing system recognition and array processing [33–36]. It is also used for sensing receiver filter design. Let an $N \times 1$ vector $\mathbf{x}$ be the IV receive filter. Thus, the IV receive filter calculates

$$\mathbf{x}^T \mathbf{y} = \alpha_0 \mathbf{x}^T \mathbf{s} + \sum_{i=-N+1, n\neq 0}^{N-1} \alpha_i \mathbf{x}^T \mathbf{J}_i \mathbf{s}. \tag{9}$$

The signal-to-clutter ratio (SCR) at the output of the IV receive filter can be defined as

$$\text{SCR}_{\text{IV}} = \frac{|\alpha_0|^2 (\mathbf{x}^T \mathbf{s})^2}{\sum_{i=-N+1, n\neq 0}^{N-1} (\alpha_i \mathbf{x}^T \mathbf{J}_i \mathbf{s})^2} = \frac{|\alpha_0|^2 (\mathbf{x}^T \mathbf{s})^2}{\mathbf{x}^T \mathbf{R} \mathbf{x}}. \tag{10}$$

In (10), $\mathbf{R} = \sum_{i=-N+1, n\neq 0}^{N-1} |\alpha_i|^2 \mathbf{J}_i \mathbf{s} \mathbf{s}^T \mathbf{J}_i^T$. Generally, $|\mathbf{R}| \neq 0$ as presented in [37]. Let $\mathbf{R}^{1/2}$ be a symmetric square root of $\mathbf{R}$. Based on the Cauchy–Schwartz inequality

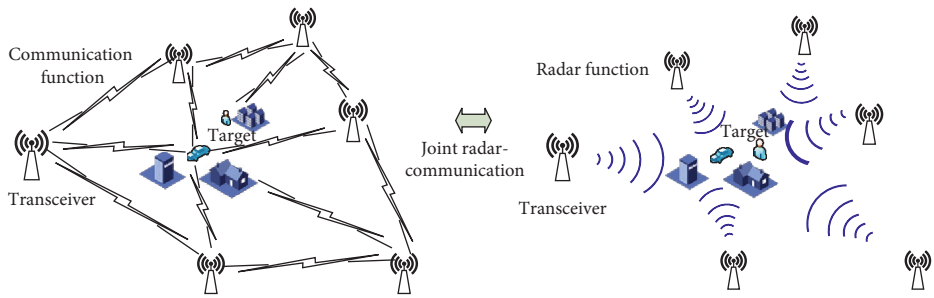

Figure 2: The joint communication-radar operation.

$(\mathbf{x}^T\mathbf{R}^{1/2}\mathbf{R}^{-1/2}\mathbf{s})^2 \le (\mathbf{x}^T\mathbf{R}\mathbf{x})(\mathbf{s}^T\mathbf{R}^{-1}\mathbf{s})$, we have $\mathrm{SCR}_{\mathrm{IV}}^{\mathrm{o}} = \max_{\mathbf{x}} \mathrm{SCR}_{\mathrm{IV}} = \mathbf{s}^T\mathbf{R}^{-1}\mathbf{s}$. The maximizing IV receive filter $\mathbf{x}$ can be expressed by $\hat{\mathbf{x}} = \mathbf{R}^{-1}\mathbf{s}$. Clearly, we can obtain $\mathrm{SCR}_{\mathrm{MF}} = \mathrm{SCR}_{\mathrm{IV}}(\mathbf{x} = \mathbf{s}) \le \mathrm{SCR}_{\mathrm{IV}}^{\mathrm{o}}$, and the equality holds if and only if $\mathbf{R}$ is equivalent to $\mathbf{I}$.

The IV receive filter method is referred to as the mismatched filtering (MMF) method as well ([34, 36] and the references therein). An important phenomenon about the IV receive filter method is that $\mathrm{SCR}_{\mathrm{IV}}^{\mathrm{o}}$ increases monotonically as the length of radar codes N increases [34]; precisely, $\mathrm{SCR}_{\mathrm{IV}}^{\mathrm{o}}(\mathbf{s}) \le \mathrm{SCR}_{\mathrm{IV}}^{\mathrm{o}}(\mathbf{s}')$, where transmit waveform $\mathbf{s}'$ denotes any coded sequence of length longer than N, which comprises $\mathbf{s}$ among its codes. The phenomenon is exploited to increase the value of $\mathrm{SCR}_{\mathrm{IV}}^{\mathrm{o}}$ prominently, without increasing complexity of the dual-function transmitter, by just adding zeros to coded sequence $\mathbf{s}$; the IV receive filter method suggests selecting coded sequence $\mathbf{s}$ as the solution to $\max_{\mathbf{s}} \mathbf{s}^T\mathbf{R}^{-1}\mathbf{s}$. Notice that, without solving $\max_{\mathbf{s}} \mathbf{s}^T\mathbf{R}^{-1}\mathbf{s}$, we utilize the IV receive filter instead of the matched filter to obtain a greater value of SCR for any $\mathbf{s}$. If the signal-independent disturbance is considered, equation (9) is rewritten as follows:

$$\mathbf{x}^T\mathbf{y} = \alpha_0\mathbf{x}^T\mathbf{s} + 2\sum_{i=1}^{N-1}\alpha_i\mathbf{x}^T\mathbf{J}_i\mathbf{s} + \mathbf{n}. \tag{11}$$

In (11), $\mathbf{n}$ denotes the $N \times 1$ vector of the filtered signal-independent disturbance samples, which is assumed to be a zero-mean colored noise $E[\mathbf{n}] = 0$ and $E[\mathbf{n}\mathbf{n}^H] = \mathbf{W} > 0$. Hence, the SCR in (10) is revised to present the signal-to-clutter-and-noise ratio (SCNR) as follows:

$$\mathrm{SCNR}_{\mathrm{IV}} = f(\mathbf{x}, \mathbf{s}) = \frac{|\alpha_0|^2(\mathbf{x}^T\mathbf{s})^2}{\mathbf{x}^T\mathbf{R}\mathbf{x} + \mathbf{x}^T\mathbf{W}\mathbf{x}}. \tag{12}$$

It is worth noting that the maximum value of (12) acquired by maximizing with regard to $\mathbf{x}$ is larger than or equal to the SCNR value using a match filter [34].

4. Problem Formulations

We consider that the prior knowledge of signal-dependent and signal-independent disturbance is known on the transmitting terminal via cognitive approaches [38]. The SCNR in (12) is considered as the performance index of the proposed DFRC system [39]. Then, we intend to obtain a joint design of the transmitted waveform and the IV receive filter. As to the shape of the code, the focus is on both continuous phase codes $|s(k)| = 1, k = 0, 1, \ldots, N-1$ and discrete phase code $s(k) \in \{1, e^{j2\pi/M}, \ldots, e^{j2\pi(M-1)/M}\}$, $k = 0, 1, \ldots, N-1$. Along with the shape constraint, a similarity constraint is imposed on the coded sequence:

$$\|\mathbf{s} - \mathbf{s}_0\|^2 \le \delta. \tag{13}$$

In (13), $\delta \ge 0$ denotes the size of the similarity region, and $\mathbf{s}_0$ signifies a specified coded sequence. By doing this, we can search for the good quality solution, which is similar to a given coded waveform $\mathbf{s}_0$. The constrained optimization of SCNR led to a coded sequence with constant modulus variations, desired range resolution, and peak sidelobe levels. Assuming that the vector of observations $\mathbf{y}$ is filtered through $\mathbf{x}$, the objective function $f(\mathbf{x}, \mathbf{s}) = (|\alpha_0|^2(\mathbf{x}^T\mathbf{s})^2/\mathbf{x}^T\mathbf{R}\mathbf{x} + \mathbf{x}^T\mathbf{W}\mathbf{x})$ is the SCNR at the output of the receive filter (obviously, we assume that $\mathbf{x} \ne 0$). Thus, we can formulate the joint design problem of the transmit coded sequence and the IV receive filter as the joint optimization problem:

$$\begin{aligned} \max_{\mathbf{s},\mathbf{x}} \quad & \frac{|\alpha_0|^2(\mathbf{x}^T\mathbf{s})^2}{\mathbf{x}^T\mathbf{R}\mathbf{x} + \mathbf{x}^T\mathbf{W}\mathbf{x}}, \\ \text{s.t.} \quad & |s(k)| = 1, \quad k = 0, 1, \ldots, N-1, \\ & \|\mathbf{s} - \mathbf{s}_0\|^2 \le \delta, \end{aligned} \tag{14}$$

for a continuous phase code and

$$\begin{aligned} \max_{\mathbf{s},\mathbf{x}} \quad & \frac{|\alpha_0|^2(\mathbf{x}^T\mathbf{s})^2}{\mathbf{x}^T\mathbf{R}\mathbf{x} + \mathbf{x}^T\mathbf{W}\mathbf{x}}, \\ \text{s.t.} \quad & s(k) \in \{1, e^{j2\pi/M}, \ldots, e^{j2\pi(M-1)/M}\} \\ & k = 0, 1, \ldots, N-1, \\ & \|\mathbf{s} - \mathbf{s}_0\|^2 \le \delta, \end{aligned} \tag{15}$$

for a discrete phase code. The joint design problems (14) and (15) are nonconvex optimization problems because the objective function is a nonconvex function and the constraints $|s(k)| = 1, k = 0, 1, \ldots, N-1$, and $s(k) \in \{1, e^{j2\pi/M}, \ldots, e^{j2\pi(M-1)/M}\}, k = 0, 1, \ldots, N-1$, define nonconvex sets. We develop sequential optimization processes, providing excellent approximate solutions for (14) and (15) with a polynomial time operational cost. The

fundamental way is to repeatedly enhance the SCNR in (12). Precisely, particularly for the IV receive filter $\mathbf{x}^{(n-1)}$at the $(n-1)$th iteration, we find a suitable coded sequence $\mathbf{s}^{(n)}$ at the nth iteration enhancing the SCNR with respect to $\mathbf{x}^{(n-1)}$ and $\mathbf{s}^{(n-1)}$ at the $(n-1)$th iteration. When $\mathbf{s}^{(n)}$ is obtained, we update the sequence and find the IV receive filter $\mathbf{x}^{(n)}$ at nth iteration which enhances the SCNR with respect to $\mathbf{s}^{(n)}$ and $\mathbf{x}^{(n-1)}$ and so on. Otherwise stated, we use $\mathbf{x}^{(n)}$ and $\mathbf{s}^{(n)}$ as the initial point at the $(n+1)$th iteration. To initiate the process, the initial filter $\mathbf{x}^{(0)}$ to a suitable coded sequence $\mathbf{s}^{(0)}$ is given. From the perspective of analysis, $\mathbf{x}^{(n)}$ denotes the optimum solution to an optimization problem, which can be expressed as

$$\max_{\mathbf{x}} \frac{\left|\alpha_0\right|^2 \left(\mathbf{x}^T \mathbf{s}^{(n)}\right)^2}{\mathbf{x}^T \mathbf{R}^{(n)} \mathbf{x} + \mathbf{x}^T \mathbf{W} \mathbf{x}}. \tag{16}$$

In (16), $\mathbf{R}^{(n)} = 2\sum_{i=1}^{N-1} |\alpha_i|^2 \mathbf{J}_i \mathbf{s}^{(n)} \mathbf{s}^{(n)T} \mathbf{J}_i^T$. According to literature [17], problem (16) is solvable. Then, for any feasible $\mathbf{s}^{(n)}$, we can obtain a closed form optimum solution $\mathbf{x}^{(n)}$. Precisely, an optimum solution to problem (14) can be written as follows:

$$\mathbf{x}^{(n)} = \frac{\left(\mathbf{R}^{(n)} + \delta_n^2 \mathbf{I}\right)^{-1} \mathbf{s}^{(n)}}{\left\| \left(\mathbf{R}^{(n)} + \delta_n^2 \mathbf{I}\right)^{-1/2} \mathbf{s}^{(n)} \right\|^2}, \tag{17}$$

from which the influence of phase coded sequence $\mathbf{s}^{(n)}$ on IV receive filter $\mathbf{x}^{(n)}$ is obvious. Moreover, phase coded sequence $\mathbf{s}^{(n)}$ can be expressed as

$$\mathbf{s}^{(n)} = \underset{\mathbf{s} \in \left\{\mathbf{s}^{(n-1)}, \mathbf{s}^{(*)}\right\}}{\arg\max} \frac{\left|\alpha_0\right|^2 \left(\mathbf{x}^{(n-1)^T} \mathbf{s}\right)^2}{\mathbf{x}^{(n-1)^T} \mathbf{R} \mathbf{x}^{(n-1)} + \mathbf{x}^{(n-1)^T} \mathbf{W} \mathbf{x}^{(n-1)}}. \tag{18}$$

In (18), $\mathbf{s}^{(*)}$ is a good solution of problem (19) if the focus is on (14) and a good solution of problem (19) if the focus is on (15), respectively, given by:

$$\begin{aligned}
\max_{\mathbf{s}} \quad & \frac{\left|\alpha_0\right|^2 \left(\mathbf{x}^{(n-1)^T} \mathbf{s}\right)^2}{\mathbf{x}^{(n-1)^T} \mathbf{R} \mathbf{x}^{(n-1)} + \mathbf{x}^{(n-1)^T} \mathbf{W} \mathbf{x}^{(n-1)}}, \\
\text{s.t.} \quad & |s(k)| = 1, \quad k = 0, 1, \ldots, N-1, \\
& \left\|\mathbf{s} - \mathbf{s}_0\right\|^2 \le \delta, \\
\max_{\mathbf{s}} \quad & \frac{\left|\alpha_0\right|^2 \left(\mathbf{x}^{(n-1)^T} \mathbf{s}\right)^2}{\mathbf{x}^{(n-1)^T} \mathbf{R} \mathbf{x}^{(n-1)} + \mathbf{x}^{(n-1)^T} \mathbf{W} \mathbf{x}^{(n-1)}}, \\
\text{s.t.} \quad & s(k) \in \left\{1, e^{j2\pi/M}, \ldots, e^{j2\pi(M-1)/M}\right\}, \quad k = 0, 1, \ldots, N-1, \\
& \left\|\mathbf{s} - \mathbf{s}_0\right\|^2 \le \delta.
\end{aligned} \tag{19}$$

Based on [14], the sequential optimization technique has some properties presented in Proposition 1.

Proposition 1: *Let $\{(\mathbf{s}^{(n)}, \mathbf{w}^{(n)})\}$ denote a sequence of points gained based on the sequential optimization technique, either for the continuous or the discrete phase code constraints; let $SCNR^{(n)}$ denote the value of SCNR with respect to the point $(\mathbf{s}^{(n)}, \mathbf{w}^{(n)})$ at the nth step. We obtain the following:*

(1) The sequence $SCNR^{(n)}$ is a monotonic increasing sequence and finally converges to an optimal value $SCNR^{(*)}$

(2) Starting from the sequence $\{(\mathbf{s}^{(n)}, \mathbf{w}^{(n)})\}$, it is possible to construct another sequence $\{(\widehat{\mathbf{s}}^{(n)}, \widehat{\mathbf{w}}^{(n)})\}$ that converges to a feasible point $(\widehat{\mathbf{s}}^{(*)}, \widehat{\mathbf{w}}^{(*)})$ of problems (14) or (15), such that the SCNR evaluated in $(\widehat{\mathbf{s}}^{(*)}, \widehat{\mathbf{w}}^{(*)})$ is equal to $SCNR^{(*)}$

In practical terms, the sequential design process needs a situation to stop the iterations. We can find some methods to impose it, such as imposing an iteration gain constraint $|SCNR^{(n)} - SCNR^{(n-1)}| \le \zeta$ or setting the maximum number of acceptable iterations or both use a two method, where ζ indicates the given threshold. In the following subsections, we are going to devote to the research of problems (19) and (20) in order to realize the sequential optimization processes.

4.1. Coded Sequence Design: Solution of (19). Based on [21], the SCNR in (12) can be expressed equivalently by $(|\alpha_0|^2 (\mathbf{s}^T \mathbf{x}^*)^2) / (\mathbf{s}^T \mathbf{R} \mathbf{x} \mathbf{s}^* + \mathbf{x}^T \mathbf{W} \mathbf{x})$. Then, a novel approach to obtain in polynomial time an approximate optimal solution to the NP-hard problem (19) is presented. We can equivalently reformulate problem (19) as follows:

$$\begin{aligned}
\max_{\mathbf{s}} \quad & \frac{\left|\alpha_0\right|^2 \left(\mathbf{s}^T \mathbf{x}^{(n-1)^*}\right)^2}{\mathbf{s}^T \mathbf{R} \mathbf{x}^{(n-1)} \mathbf{s}^* + \mathbf{x}^{(n-1)^T} \mathbf{W} \mathbf{x}^{(n-1)}}, \\
\text{s.t.} \quad & |s(k)| = 1, \quad k = 0, 1, \ldots, N-1, \\
& \left\|\mathbf{s} - \mathbf{s}_0\right\|^2 \le \delta.
\end{aligned} \tag{20}$$

Observe that problem (20) is a nonconvex fractional quadratic problem [21]. Because $|s(k)| = |s_0(k)| = 1, k = 0, 1, \ldots, N-1$, an equivalent expression of the similarity constraint $\max_{k \in [1,\ldots,N]} |s(k) - s_0(k)| \le \delta$ is expressed by $\Re[s^*(k) s_0(k)] \ge 1 - (\delta^2/2)$for $k = 0, 1, \ldots, N-1$, which can be equivalent to enforcing $\arg(s(k)) \in [\gamma_k, \gamma_k + \delta_c]$, where $\gamma_k = \arg(s_0(k)) - \arccos(1 - (\delta^2/2))$ and $\delta_c = 2\arccos(1 - \delta^2/2)$ for $k = 0, 1, \ldots, N-1$ [30]. Therefore, NP-hard problem (20) can be rewritten as

$$\begin{aligned}
\max_{\mathbf{s}} \quad & \frac{\left|\alpha_0\right|^2 \left(\mathbf{s}^T \mathbf{x}^{(n-1)^*}\right)^2}{\mathbf{s}^T \mathbf{R} \mathbf{x}^{(n-1)} \mathbf{s}^* + \mathbf{x}^{(n-1)^T} \mathbf{W} \mathbf{x}^{(n-1)}}, \\
\text{s.t.} \quad & |s(k)| = 1, \quad k = 0, 1, \ldots, N-1, \\
& \arg(s(k)) \in [\gamma_k, \gamma_k + \delta_c], k = 0, 1, \ldots, N-1.
\end{aligned} \tag{21}$$

Noting that (21) is generally an NP-hard problem, it is difficult to find optimal solutions for (21) with a polynomial time calculation burden. We present approximate optimization approaches and develop a semidefinite programming (SDP) relaxation and randomization technique that offers an expected feasible solution to (21). Let $\mathbf{Y} = \mathbf{x}^{(n-1)}\mathbf{x}^{(n-1)^T}$ and $\mathbf{M} = \mathbf{R}(\mathbf{x}^{(n-1)})^* + (\delta_n^2/N)\|\mathbf{x}^{(n-1)}\|^2\mathbf{I}$. Therefore, the relaxed version of NP-hard problem (21), acquired ignoring the similarity constraint $\arg(s(k)) \in [\gamma_k, \gamma_k + \delta_c], k = 0, 1, ..., N-1$, can be expressed as

$$\begin{aligned} \max_{\mathbf{s}} \quad & \frac{|\alpha_0|^2\left(\mathbf{s}^T\mathbf{x}^{(n-1)^*}\right)^2}{\mathbf{s}^T\mathbf{R}\mathbf{x}^{(n-1)}\mathbf{s}^* + \mathbf{x}^{(n-1)^T}\mathbf{W}\mathbf{x}^{(n-1)}}, \\ \text{s.t.} \quad & |s(k)| = 1, \quad k = 0, 1, ..., N-1. \end{aligned} \tag{22}$$

The fractional quadratic problem (22) can be expressed equivalently as

$$\begin{aligned} \max_{\mathbf{X},\mathbf{s}} \quad & \frac{\mathrm{tr}(\mathbf{YS})}{\mathrm{tr}(\mathbf{MS})}, \\ \text{s.t.} \quad & |\mathbf{S}(k,k)| = 1, \quad k = 0, 1, ..., N-1, \\ & \mathbf{S} = \mathbf{s}\mathbf{s}^T. \end{aligned} \tag{23}$$

The SDP [40] of (23), acquired dropping the rank-one constraint $\mathbf{S} = \mathbf{s}\mathbf{s}^T$, can be denoted as

$$\begin{aligned} \max_{\mathbf{X},\mathbf{s}} \quad & \frac{\mathrm{tr}(\mathbf{YS})}{\mathrm{tr}(\mathbf{MS})}, \\ \text{s.t.} \quad & |\mathbf{S}(k,k)| = 1, \quad k = 0, 1, ..., N-1, \\ & \mathbf{S} \succ 0. \end{aligned} \tag{24}$$

According to literature [41], to find an optimal solution to (24), it is sufficient to solve the equivalent SDP problem:

$$\begin{aligned} \max_{\mathbf{X},\mathbf{s}} \quad & \mathrm{tr}(\mathbf{YS}), \\ \text{s.t.} \quad & \mathrm{tr}(\mathbf{MS}) = 1 \\ & \mathbf{S}(k,k) = u \\ & \mathbf{S} \succ 0. \end{aligned} \tag{25}$$

Let us observe that both (24) and (25) are solvable and have equivalent optimal solution; actually, if $(\widehat{\mathbf{S}}, \widehat{u})$ solves (25), then we can easily and clearly find out $\widehat{\mathbf{S}}/\widehat{u}$ is an optimal solution of (24); similarly, if $\widehat{\mathbf{S}}$ solves (24), then $(\widehat{\mathbf{S}}/\mathrm{tr}(\mathbf{M}\widehat{\mathbf{S}}), 1/\mathrm{tr}(\mathbf{M}\widehat{\mathbf{S}}))$ is an optimal solution of (25). Consequently, resorting to the scheme as presented in [30], we can find an expected feasible solution $\mathbf{s}^*$ to (19) by using Algorithm 1 where the parameter L indicates the number of Randomizations.

The complexity, corresponding to the operation of Algorithm 1, is relative to the complexity required to solve a SDP problem $O(N^{3.5})$, whereas all randomizations involve $O(N^2)$ [21].

4.2. Coded Sequence Design: Solution of (20). At present, many sensing systems transmit phase coded sequences, where the phases are chosen from a finite alphabet. Consequently, we present a novel approach to obtain in polynomial time approximate optimal solutions to the NP-hard problem (20). We consider that $s_0(k) \in \{1, e^{j2\pi/M}, ..., e^{j2\pi(M-1)/M}\}, k = 0, 1, ..., N-1$ where $M \geq 2$, if $M = 2$ and $\delta < 2$ and the optimal solution to (20) is the trivial one $\mathbf{s}^* = \mathbf{s}_0$. Thus, based on [21], (20) can be expressed equivalently as follows:

$$\begin{aligned} \max_{\mathbf{s}} \quad & \frac{|\alpha_0|^2\left(\mathbf{s}^T\mathbf{x}^{(n-1)^*}\right)^2}{\mathbf{s}^T\mathbf{R}\mathbf{x}^{(n-1)}\mathbf{s}^* + \mathbf{x}^{(n-1)^T}\mathbf{W}\mathbf{x}^{(n-1)}}, \\ \text{s.t.} \quad & s(k) \in \left\{1, e^{j2\pi/M}, ..., e^{j2\pi(M-1)/M}\right\} \\ & k = 0, 1, ..., N-1, \\ & \left\|\mathbf{s} - \mathbf{s}_0\right\|_\infty \leq \delta. \end{aligned} \tag{26}$$

Let us observe that problem (26) is a nonconvex fractional quadratic problem as well. Since $\{s(k), s_0(k)\} \in \left\{1, e^{j2\pi/M}, ..., e^{j2\pi(M-1)/M}\right\}^2$, $k = 0, 1, ..., N-1$, an equivalent expression of the similarity constraint $\max_{k\in[1,...,N]}|s(k) - s_0(k)| \leq \delta, k = 0, 1, ..., N-1$ is denoted by $\Re[s^*(k)s_0(k)] \geq 1 - (\delta^2/2)$ for $k = 0, 1, ..., N-1$, which in turn equals to imposing $s(k) \in \{e^{j2\pi(\beta k/M)}, e^{j2\pi((\beta k+1)/M)}, ..., e^{j2\pi((\beta k+\delta d-1)/M)}\}$, where $\beta_k = M\arg(s_0(k))/2\pi - M\arccos(1-\delta^2/2)/2\pi$ for $k = 0, 1, ..., N-1$ and $\delta_d = \begin{cases} 1 + 2\lfloor(\arccos(1-\delta^2/2)/2\pi)\rfloor, & \delta \in [0, 2) \\ M, & \delta = 2 \end{cases}$. Therefore, NP-hard problem (26) can be rewritten as

$$\begin{aligned} \max_{\mathbf{s}} \quad & \frac{|\alpha_0|^2\left(\mathbf{s}^T\mathbf{x}^{(n-1)^*}\right)^2}{\mathbf{s}^T\mathbf{R}\mathbf{x}^{(n-1)}\mathbf{s}^* + \mathbf{x}^{(n-1)^T}\mathbf{W}\mathbf{x}^{(n-1)}}, \\ \text{s.t.} \quad & \arg(s(k)) \in \frac{2\pi}{M}\left[\beta_k, \beta_k + 1, ..., \beta_k + \delta_d - 1\right] \\ & |s(k)| = 1, \; k = 0, 1, ..., N-1. \end{aligned} \tag{27}$$

Notice that (21) is generally NP-hard problem as well, subsequently it is difficult to obtain polynomial time procedures for calculating optimal solutions to (21). We present approximate optimization approaches and develop a semidefinite programming (SDP) relaxation and randomization technique that offers an expected feasible solution to (27). Therefore, based on $\mathbf{Y}$ and $\mathbf{M}$ discussed above, making use of the similar relaxation technique as stated in (22)–(25) and resorting to the similar stages as presented in [30], we can obtain an expected feasible solution $\mathbf{s}^*$ to (20) by using Algorithm 2.

Similar to Algorithm 1, the function of the L randomizations is to enhance the approximate capacity;

Input: The parameters $\mathbf{M}$, $\mathbf{Y}$, L, $\{\gamma_k\}$,δ_c
Output: An approximation solution $\mathbf{s}^*$ to Problem (19)
Step 1: Calculate the optimal solution $(\mathbf{S}^*, u^*)$ of SDP Problem (25)
Step 2: Define $\widehat{\mathbf{S}} = \mathbf{S}^*/u^*$
Step 3: Produce random vectors $(\boldsymbol{\xi})_i \in \mathbb{C}^N, i = 1, ..., L$, from the normal distribution $N_{\mathbb{C}}(0, \mathbf{Z})$ where $\mathbf{Z} = \widehat{\mathbf{S}} \odot \mathbf{z}_c \mathbf{z}_c^T$ and $\mathbf{z}_c = [e^{j\gamma 1}, ..., e^{j\gamma N}]^T$
Step 4: Let $(s(k))_i = y_c^*(k)\delta((\xi_k)_i), k = 1, ..., N, i = 1, ..., L$, where $\delta(x) = e^{(j\arg(x)/2\pi)\delta_c}, x \in \mathbb{C}$
Step 5: Calculate $t_i = (\mathbf{s}_i^T \mathbf{Y} \mathbf{s}_i / \mathbf{s}_i^T \mathbf{M} \mathbf{s}_i), i = 1, ..., L$
Step 6: Choice the greatest value over $\{t_1, ..., t_L\}$ say t_1, **output** $\mathbf{s}^* = \mathbf{s}_1$

Algorithm 1: An approximation algorithm for the continuous phase code using the SDP relaxation technique.

Input: The parameters $\mathbf{M}$, $\mathbf{Y}$, L, $\{\beta_k\}$, δ_d,M
Output: An approximation solution $\mathbf{s}^*$ to Problem (20)
Step 1: Let $(\mathbf{S}^*, u^*)$ be an optimum solution to SDP Problem (25)
Step 2: Define $\widehat{\mathbf{S}} = \mathbf{S}^*/u^*$
Step 3: Produce random vectors $(\boldsymbol{\xi})_i \in \mathbb{C}^N, i = 1, ..., L$, from the normal distribution $N_{\mathbb{C}}(0, \mathbf{W})$ where $\mathbf{W} = \widehat{\mathbf{S}} \odot \mathbf{z}_d \mathbf{z}_d^T$ and $\mathbf{z}_d = [e^{j(2\pi/M)\beta_1}, ..., e^{j(2\pi/M)\beta_N}]^T$
Step 4: Let $(s(k))_i = y_d^*(k)\delta((\xi_k)_i), k = 1, ..., N, i = 1, ..., L$, where $\mu(x) = \begin{cases} 1, & \text{if } \arg x \in [0, 2\pi(1/\delta_d)) \\ e^{j2\pi(1/M)}, & \text{if } \arg x \in [2\pi(1/\delta_d), 2\pi(2/\delta_d)) \\ \cdots & \\ e^{j2\pi((\delta_d - 1)/M)}, & \text{if } \arg x \in [2\pi(\delta_d - 1/\delta_d), 2\pi) \end{cases}$
Step 5: Calculate $t_i = (\mathbf{s}_i^T \mathbf{Y} \mathbf{s}_i / \mathbf{s}_i^T \mathbf{M} \mathbf{s}_i), i = 1, ..., L$
Step 6: Choice the greatest value over $\{t_1, ..., t_L\}$ say t_1, **output** $\mathbf{s}^* = \mathbf{s}_1$

Algorithm 2: An approximation algorithm for the discrete phase code using the SDP relaxation technique.

furthermore, the overall complexity of Algorithm 2 is relative to the approximation solution of SDP relaxation $O(N^{3.5})$.

4.3. Coded Sequence-IV Receive Filter Design. We summarize the sequential optimization techniques for the coded sequence and the IV receive filter, separately, as Algorithm 3 for the continuous phase constraint and Algorithm 4 for the discrete phase constraint. To generate the iteration, an initial coded sequence $\mathbf{s}^{(0)}$, from which we can acquire the suitable IV receive filter $\mathbf{w}^{(0)}$, is necessary; a regular set is apparently $\mathbf{s}^{(0)} = \mathbf{s}_0$.

The complexity, corresponding to the operation of Algorithms 3 and 4, depends on the maximum number of acceptable iterations $\widehat{N}$ along with on and the computational complexity involved in all iterations. Specifically, the overall computational complexity is linear in regard to $\widehat{N}$, while in all iterations, they contain the computation of the inverse of $\mathbf{R}^{(0)} + \delta_n^2 \mathbf{I}$ and the complexity effort of Algorithms 1 and 2, separately. The former is in the order of $O(N^3)$. The latter, for a reasonable number of randomizations, is relative to the complexity required to solve a SDP $O(N^{3.5})$ [21].

5. Performance Analysis

In this section, the capability provided by the constrained optimization techniques for the design of the coded sequence and the IV receiver is evaluated. Numerical results based on Monte Carlo simulations are offered to verify the effectiveness of the constrained optimization techniques. We assume a DFRC system operating in the X-band with carrier frequency $f_c = 8.2$ GHz and bandwidth $B = 500$ MHz. The sampling frequency is $f_s = 10^9$ sample/sec. Furthermore, we assume the length of the coded sequence $N = 20$ and choose, as similarity coded sequence $\mathbf{s}_0$, the N-dimensional generalized Barker codes and the M-quantized coded sequence for Algorithms 3 and 4, separately. Precisely, prearranging the coded sequence $\mathbf{s}$, we generate the M-quantized coded sequence $\mathbf{s}^q$, which is given by $s^q(k) = \overline{\mu}(s(k)), k = 1, ..., N$, where $\overline{\mu}(x)$ is the nonlinearity, which is denoted as follows:

$$\overline{\mu}(x) = \begin{cases} 1, & \text{if } \arg x \in \left[0, 2\pi\dfrac{1}{M}\right), \\ e^{j2\pi(1/M)}, & \text{if } \arg x \in \left[2\pi\dfrac{1}{M}, 2\pi\dfrac{2}{M}\right), \\ \cdots & \\ e^{j2\pi((M-1)/M)}, & \text{if } \arg x \in \left[2\pi\dfrac{M-1}{M}, 2\pi\right). \end{cases} \tag{28}$$

In regard to the continuous phase code, the use of the similarity coded sequence is primarily owing to its autocorrelation properties. The explanation of the generalized Barker code has been presented in [21], which contains various length values. We consider that the randomizations in Algorithms 1 and 2 is $L = 150$. The exit condition in Algorithms 3 and 4 assumes $\xi = 10^{-5}$, viz.

Input: The parameters $\mathbf{s}_0$, L, δ, ξ,δ_n^2
Output: An approximate solution $(\mathbf{s}^*, \mathbf{x}^*)$ of Problem (14)
Step 1: Initialize $n = 0$, $\mathbf{s}^{(n)} = \mathbf{s}_0$, $\mathbf{x}^{(n)} = ((\mathbf{R}^{(0)} + \delta_n^2\mathbf{I})^{-1}\mathbf{s}_0/\|(\mathbf{R}^{(0)} + \delta_n^2\mathbf{I})^{-1/2}\mathbf{s}_0\|^2)$, $\mathrm{SCNR}^{(\mathrm{n})} = \mathrm{SCNR}$
Step 2: **do**
Step 3: $n = n + 1$
Step 4: Let $\mathbf{Y} = \mathbf{x}^{(n-1)}\mathbf{x}^{(n-1)^T}$; $\mathbf{M} = \mathbf{R}(\mathbf{x}^{(n-1)})^* + \delta_n^2\|\mathbf{x}^{(n-1)}\|^2\mathbf{I}$; Set $\{\gamma_k\}$, δ_c
Step 5: Obtain an approximate optimal solution $\mathbf{s}^*$ to (19) using Algorithm 1
Step 6: Calculate $\mathbf{s}^{(n)} = \arg\max_{\mathbf{s}\in\{\mathbf{s}^{(n-1)},\mathbf{s}^{(*)}\}} (|\alpha_0|^2(\mathbf{x}^{(n-1)^T}\mathbf{s})^2/\mathbf{x}^{(n-1)^T}\mathbf{R}\mathbf{x}^{(n-1)} + \mathbf{x}^{(n-1)^T}\mathbf{W}\mathbf{x}^{(n-1)})$
Step 7: Construct $\mathbf{R}^{(n)}$
Step 8: Calculate $\mathbf{x}^{(n)} = ((\mathbf{R}^{(n)} + \delta_n^2\mathbf{I})^{-1}\mathbf{s}^{(n)}/\|(\mathbf{R}^{(n)} + \delta_n^2\mathbf{I})^{-1/2}\mathbf{s}^{(n)}\|^2)$ and the SCNR value for $(\mathbf{s}^{(n)}, \mathbf{x}^{(n)})$
Step 9: Let $\mathrm{SCNR}^{(\mathrm{n})} = \mathrm{SCNR}$
Step 10: **until** $|\mathrm{SCNR}^{(\mathrm{n})} - \mathrm{SCNR}^{(\mathrm{n}-1)}| \le \varsigma$
Step 11: Obtain $\mathbf{s}^* = \mathbf{s}^{(n)}$; $\mathbf{x}^* = \mathbf{x}^{(n)}$

Algorithm 3: The sequential optimization Algorithm 3.

Input: The parameters $\mathbf{s}_0$, L, δ, ξ, δ_n^2, M
Output: An approximate solution $(\mathbf{s}^*, \mathbf{x}^*)$of Problem (15)
Step 1: Initialize $n = 0$, $\mathbf{s}^{(n)} = \mathbf{s}_0$, $\mathbf{x}^{(n)} = (\mathbf{R}^{(0)} + \delta_n^2\mathbf{I})^{-1}\mathbf{s}_0/\|(\mathbf{R}^{(0)} + \delta_n^2\mathbf{I})^{-1/2}\mathbf{s}_0\|^2$, $\mathrm{SCNR}^{(n)} = \mathrm{SCNR}$
Step 2: **do**
Step 3: $n = n + 1$
Step 4: Let $\mathbf{Y} = \mathbf{x}^{(n-1)}\mathbf{x}^{(n-1)^T}$; $\mathbf{M} = \mathbf{R}(\mathbf{x}^{(n-1)})^* + \delta_n^2\|\mathbf{x}^{(n-1)}\|^2\mathbf{I}$; Set $\{\beta_k\}$, δ_d
Step 5: Obtain an approximate optimal solution $\mathbf{s}^*$ to (20) using Algorithm 2
Step 6: Calculate $\mathbf{s}^{(n)} = \arg\max_{\mathbf{s}\in\{\mathbf{s}^{(n-1)},\mathbf{s}^{(*)}\}} (|\alpha_0|^2(\mathbf{x}^{(n-1)^T}\mathbf{s})^2/\mathbf{x}^{(n-1)^T}\mathbf{R}\mathbf{x}^{(n-1)} + \mathbf{x}^{(n-1)^T}\mathbf{W}\mathbf{x}^{(n-1)})$
Step 7: Construct $\mathbf{R}^{(n)}$
Step 8: Calculate $\mathbf{x}^{(n)} = (\mathbf{R}^{(n)} + \delta_n^2\mathbf{I})^{-1}\mathbf{s}^{(n)}/\|(\mathbf{R}^{(n)} + \delta_n^2\mathbf{I})^{-1/2}\mathbf{s}^{(n)}\|^2$ and the SCNR value for $(\mathbf{s}^{(n)}, \mathbf{x}^{(n)})$
Step 9: Let $\mathrm{SCNR}^{(\mathrm{n})} = \mathrm{SCNR}$
Step 10: **until** $|\mathrm{SCNR}^{(\mathrm{n})} - \mathrm{SCNR}^{(\mathrm{n}-1)}| \le \varsigma$
Step 11: Obtain $\mathbf{s}^* = \mathbf{s}^{(n)}$; $\mathbf{x}^* = \mathbf{x}^{(n)}$

Algorithm 4: The sequential optimization Algorithm 4.

$|\mathrm{SCNR}^{(n)} - \mathrm{SCNR}^{(n-1)}| \le 10^{-5}$. Furthermore, we assume the presence of a radar target with $|\alpha_T|^2 = 10$ dB. The performance evaluation is performed in terms of the achievable SCNR, with respect to the optimal coded sequence and IV filter, as well as the target detection probability. The convex optimization problems and SDP relaxation are solved via the MATLAB toolbox [42].

Figure 3 illustrates the value of the SCNR averaged over 250 independent repeated experiments of Algorithm 3 versus the number of acceptable iterations, for diverse values of the parameter $\delta = [0.1, 0.4, 1, 1.5, 1.7]$. In Figure 3, as the similarity constraint parameter δ increases, the maximum SCNR value enhances since the feasible set of the joint design scheme becomes greater and greater. In fact, for $\delta = 1.7$, performance gains generated by Algorithm 3 is 15 dB, as compared with 13 dB offered by the joint design approach as presented in [21], 11 dB by the cognition on transmitter only, and 10 dB by the cognition on receive filter only. Evidently, these are just theoretical results. In practical terms, the smaller value of the SCNR is observed because of various imprecisions in the obtainable observation.

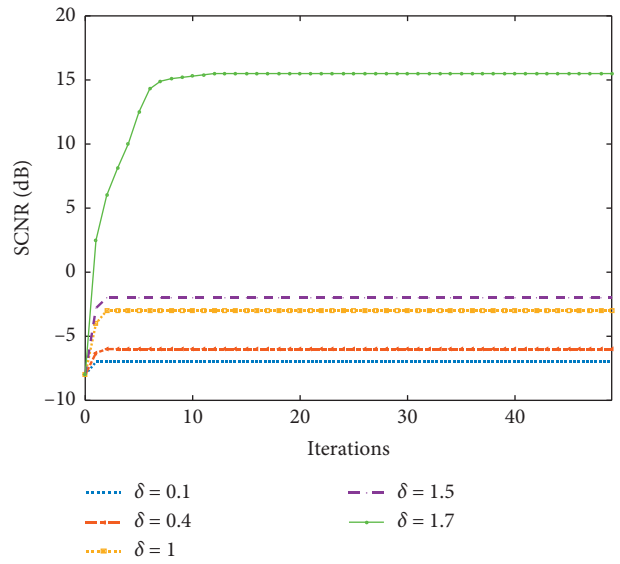

Figure 3: SCNR vs. number of iterations for continuous phase waveform.

Performance gains offered by Algorithm 3 converge after fifteen iterations, yielding 15 dB at $\delta = 1.7$ as compared with −2 dB at the beginning of the iteration. The performance gains of Algorithm 3 are improving as the number of iterations increases. However, there is an inappreciable amount of performance improvement after ten iterations.

Figure 4 demonstrates the value of the SCNR averaged over 250 independent repeated experiments of Algorithm 4 versus the number of acceptable iterations, for diverse values of $\delta = [0.1, 0.4, 1, 1.5, 1.7, 2]$ and the quantization levels $M = 16$. To discuss the results, we can use the similar explanations as in Figure 3. As can be seen from Figure 4, as the similarity constraint parameter δ increases, the bigger and bigger SCNR values are obtained through iterative operations, due to the enlargement of the feasible set of the joint optimization scheme. Indeed, for $\delta = 2$, performance gains generated by Algorithm 4 is 4 dB, as compared with 2 dB offered by the joint design approach as presented in [21], 1 dB by the cognition on transmitter only, and 0.5 dB by the cognition on receive filter only.

Figure 5 shows the attained average SCNR versus the number of acceptable iterations for $\delta = 2$ and several values of the number of quantization levels $M\,(M \in \{2, 4, 8, 16, 32\})$. We study the impacts of M on the optimized coded sequence for $\delta = 2$. As we can see from Figure 5, the result demonstrates that the greater the number of quantization levels is, the better the attained average SCNR will be until $M \geq 32$. That is to say, the better the cardinality of the alphabet, the larger the degrees of freedom obtainable in the selection of the PM-based FH codes. These results can be expected, and this is the saturation effect. The performance gains of the phase-quantized sequence offered by Algorithm 4 end up consistent with that produced by Algorithm 3.

We analyze detection performance of the optimal coded sequence and IV receive filter generated by Algorithm 3. The probability of target detection P_d versus SCNR, for some values of $\delta = [0.1, 0.5, 1, 1.5, 2, 2.5]$, is demonstrated in Figure 6. Figure 6 displays that greater the parameter δ leads to better detection performance. The result can be expected, since increasing the parameter δ results in less restriction on coded sequence and IV receive filter design, which amounts to increasing the size of the optimal solutions of the joint optimization problem.

Figure 7 describes the detection levels P_d versus SCNR, for $\delta = 1$ and the values of the number of randomizations $L \in \{1, 10, 20, 40\}$. We analyze the impact of L on P_d of the optimal coded sequence and IV receive filter offered by Algorithm 3. In Figure 7, P_d is importantly improved by enlarging the parameter L. The result is explicated through Algorithm 1, which finds the optimal coded sequence and IV receive filter assuring the excellent detection ability among all the L simulations. An indiscernible amount of capability enhancement is observed when $L \geq 10$. The detection ability is viewed acceptable. Consequently, we choose suitable value of L resulting in advisable enhancements in the detection levels.

In Figure 8, we analyze the similar performance stated in Figure 6 with regard to the detection levels P_d of the optimal

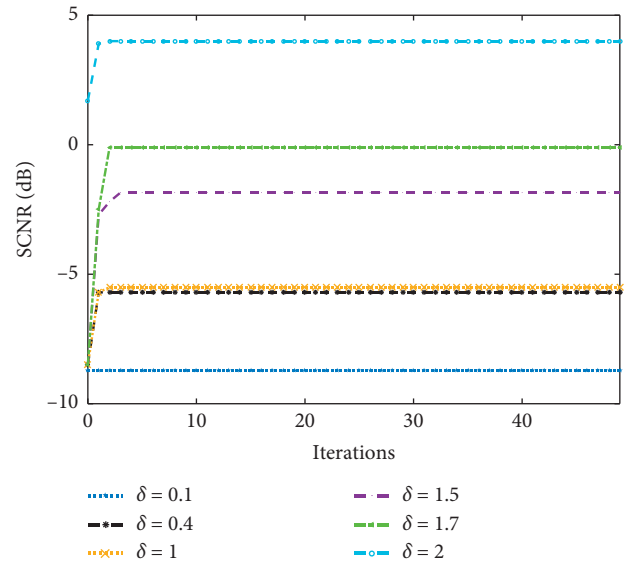

Figure 4: SCNR vs. number of iterations for phase quantized waveform.

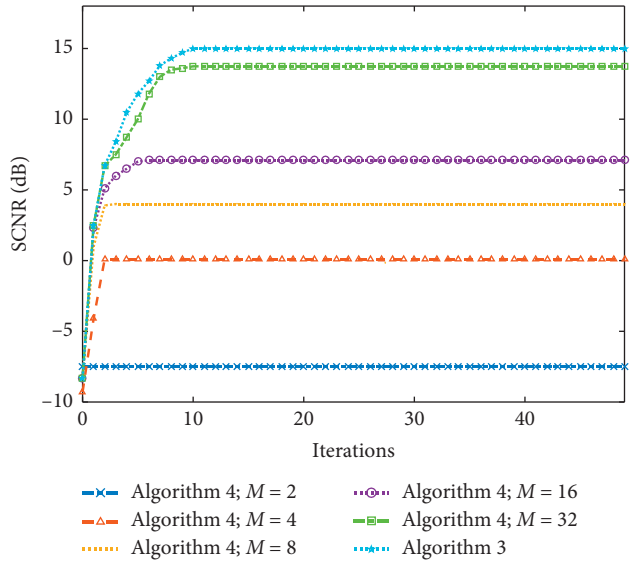

Figure 5: SCNR vs. number of iterations. Algorithm 4: phase quantized sequence. Algorithm 3: continuous phase sequence.

phase quantized sequence and IV receive filter provided by Algorithm 4. Figure 8 explains P_d of Algorithm 4 versus SCNR for some values of $\delta \in \{0.1, 0.5, 1, 1.5, 2, 2.5\}$ and quantization levels $M = 8$. Similar to Algorithm 3, as the value of δ becomes greater, P_d of the optimal phase-quantized sequence and IV receive filter provided by Algorithm 4 improved.

Figure 9 displays the performance of target detection P_d versus SCNR for $\delta = 1$ and several values of the number of quantization levels $M\,(M \in \{4, 8, 16, 32\})$. We analyze the performance of the optimal phase-quantized coded sequence and IV receive filter generated by Algorithm 4 and discuss the impact of the parameter M on the probabilityP_d. In Figure 9, this result demonstrates that the larger the

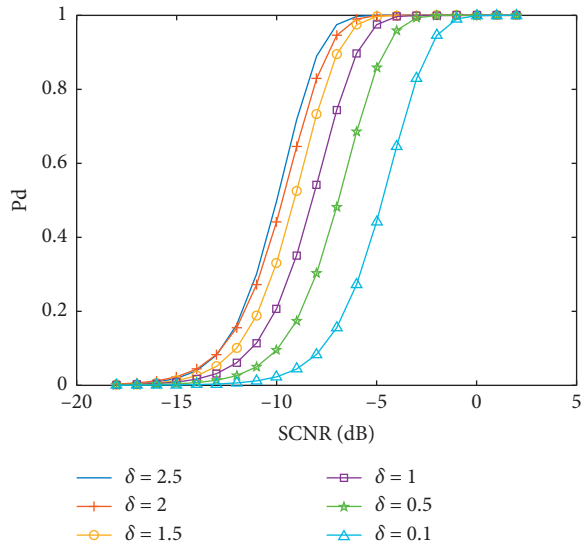

Figure 6: Detection probability vs. SCNR. Algorithm 3: continuous phase sequence.

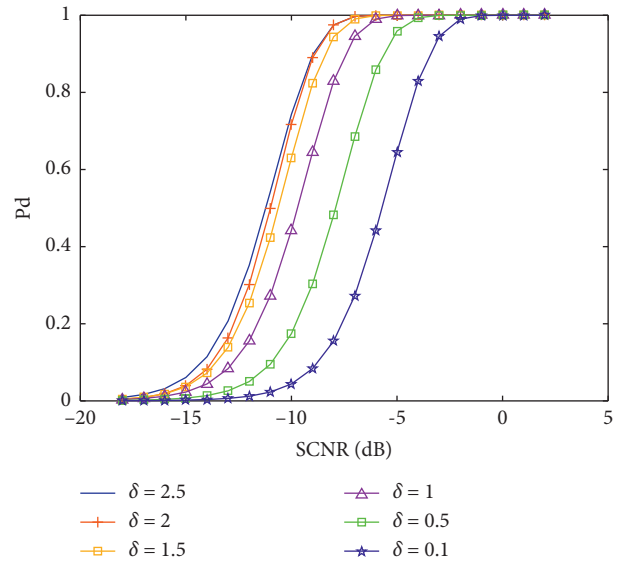

Figure 8: Detection probability versus SCNR. Algorithm 4: phase-quantized sequence.

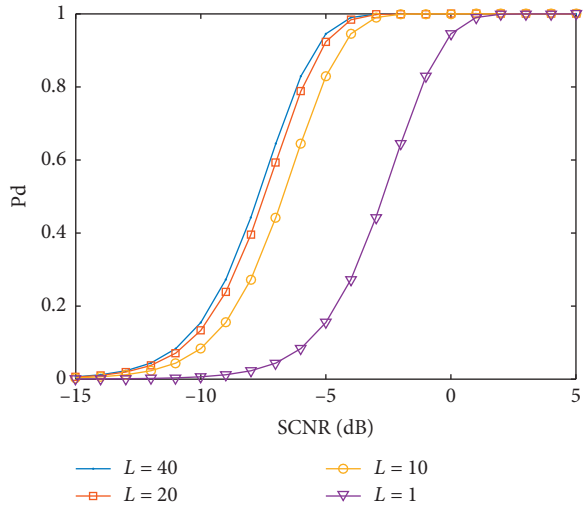

Figure 7: Detection probability versus SCNR. Algorithm 3 for same values of randomizations.

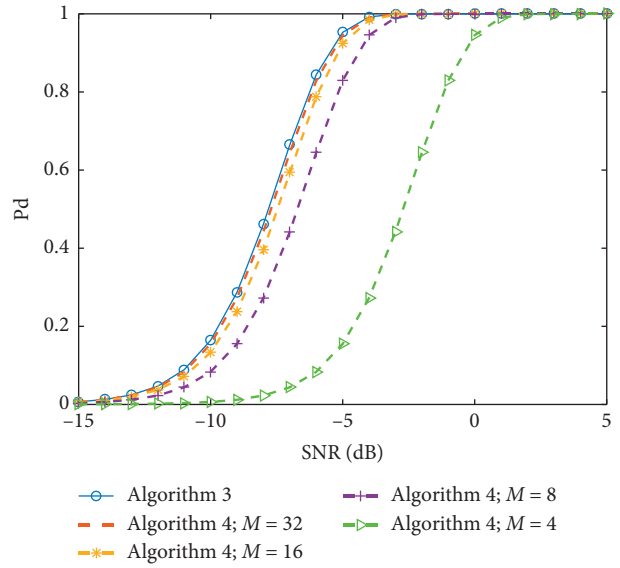

Figure 9: Detection probability versus SCNR. Algorithm 4: dashed curves. Algorithm 3: o-marked curve.

parameter M is, the improved the performance of target detection will be until $M \geq 8$. This conclusion is considered as the saturation effect. The performance of the optimal phase quantized coded sequence and IV receive filter generated by Algorithm 4 ends up consistent with that provided by Algorithm 3.

To implement the communication function, we assume that the FH step is $\Delta f = 10$ MHz, the length of the FH code is $Q = 20$, and the FH interval duration is $\Delta t = 0.1\,\mu$s. We generate a 16 FH coded sequence. The parameter $J = 50$ is used. Therefore, the 320 FH code is generated randomly from the set $\{1, 2, \ldots, J\}$, where $J = 50$.

In Figure 10, we compare the symbol error rate (SER) performance for the optimized waveform offered by Algorithm 3 with a random waveform using BPSK, QPSK, 16-PSK, and 256-PSK constellations. The data rates of the abovementioned four types of signals are 1.2, 2.4, 4.8, and 9.6 Mbps, respectively. To investigate the SER performance, 14×10^7 random PM-based FH symbols have been generated. Figure 10 illustrates the SER performance versus SNR for BPSK, QPSK, 16-PSK, and 256-PSK constellation.

Figure 10 indicates that the SER performance of BPSK random waveform is enhanced by about 5 dB, 16 dB, and 33 dB as compared with QPSK, 16-PSK, and 256-PSK random waveform, respectively. Meanwhile, as we can see from Figure 10, for BPSK, QPSK, and 16-PSK, the SER performances of the optimized waveform offered by Algorithm 3 are as good as those of random waveform. However, for the 256-PSK, the SER performance of the optimized waveform is poor relatively. As the size of constellations

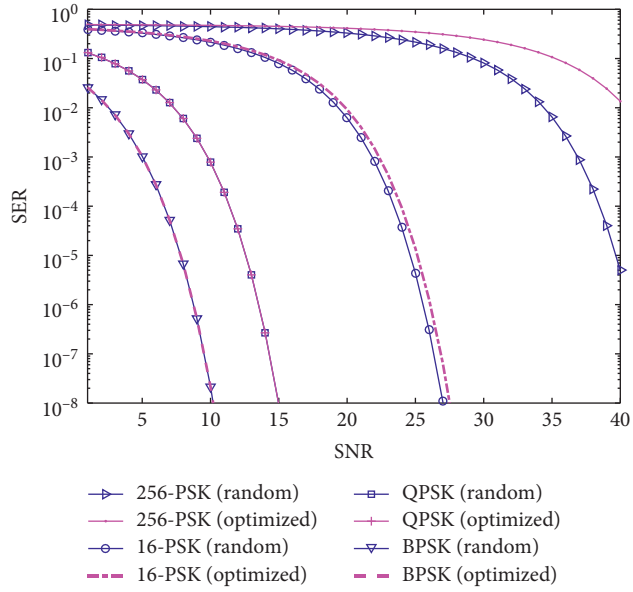

Figure 10: Comparative SER performance of BPSK, QPSK, 16-PSK, and 256-PSK.

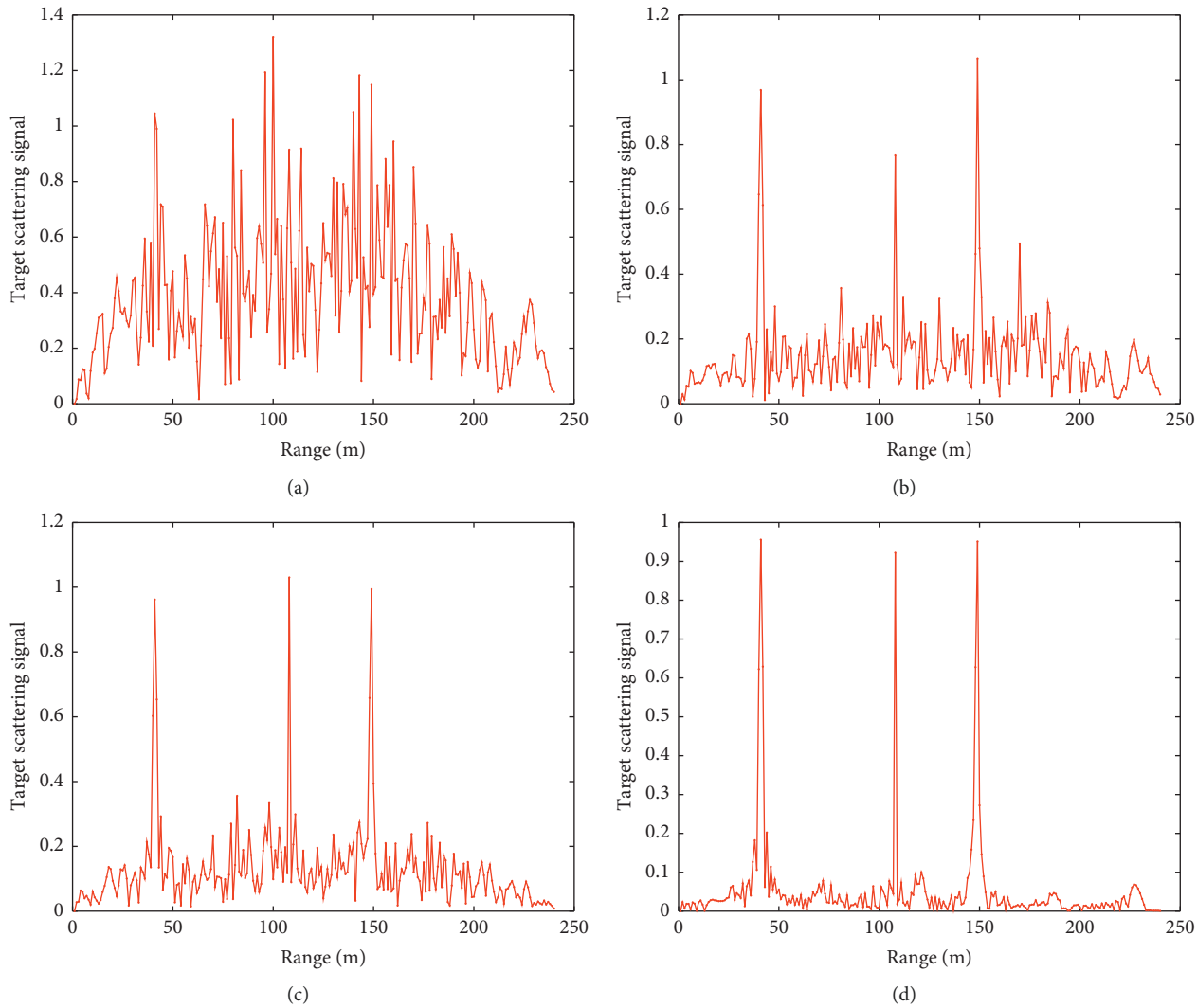

Figure 11: Target scattering signals profiles at (a) iteration 1, (b) iteration 5, (c) iteration 10, and (d) iteration 20, Algorithm 3.

increases, the cross correlation levels between the optimized waveform offered by Algorithm 3 becomes higher. As a result, to meet the more reasonable requirement mentioned above, we select suitable constellation size leading to a tradeoff between communication SER performance and data rate.

Transmit waveform design under a detection constraint is stated in some works [43, 44]. The problem of code optimization for target recognition in the presence of clutter interference is addressed. The purpose of the objective function is to optimize the Euclidean distance between the theoretical radar return from diverse target feature models. Moreover, the detection constraint involves that the attainable SCNR for all target feature models are greater than the given threshold.

Figure 11 indicates the detection variation of Algorithm 3 under the similarity constraint. We assume a radar scene, which has three targets. The target scattering signals derived from the radar scene is normalized and the dual-function complexity system intends to discriminate the scatterers by using a particular detection threshold.

With subsequent iterations of Algorithm 3, the detection performance of the multiple targets is enhanced. As can be seen from Figure 11, by suppressing noise, the dual-function complexity system could discriminate three scatterers effectively at the end of 20 iterations. The constrained joint optimization technique is superior to the waveform optimization scheme in [43]. By increasing the number of iterations, we can obtain more accurate estimates of the target responses, which are used to improve detection of the multiple targets.

6. Conclusions

In this paper, we developed the joint optimization design of cognitive radar waveform and IV receivers for the DFRC system. We presented a novel scheme trying to maximize the SCNR while accounting for a similarity constraint on the transmission phase code. At all iterations, the proposed processes involve the solution of both convex and NP-hard problems. In order to obtain an optimal solution, we turned to relaxation and randomization methods. The usefulness of the constrained optimization techniques was verified by offering simulation results. The capability of the proposed approaches in terms of achieved SCNR, detection levels, and detection variation of the coded sequence and IV filter pair was evaluated. In addition, pertaining to the discrete phase code, the influence of the quantization level on the radar capability was investigated. The complexity, corresponding to the operation of the proposed Algorithms, depends on the maximum number of acceptable iterations along with on and the computational complexity involved in all iterations. The dual-function complexity system could create an integrated platform for unmanned vehicle applications for which both situational awareness and construction of information links are important. Potential future study will focus on the joint design of the probing coded sequence and the corresponding IV filter bank optimizing the worst-case SCNR over the unknown number of lost return echo samples (eclipsing conditions), under an energy constraint and a similarity constraint.

Data Availability

The MATLAB figure data used to support the findings of this study are included within the article.

Conflicts of Interest

The authors declare no conflicts of Interest.

Acknowledgments

This work was supported by the National Natural Science Foundation of China (61761019, 61861017, 61861018, and 61862024), the Natural Science Foundation of Jiangxi Province (Jiangxi Province natural Science Fund) (20181BAB211014 and 20181BAB211013), and the Foundation of Jiangxi Educational Committee of China (GJJ180352).

References

[1] D. Ciuonzo, A. De Maio, G. Foglia, and M. Piezzo, "Intrapulse radar-embedded communications via multiobjective optimization," *IEEE Transactions on Aerospace and Electronic Systems*, vol. 51, no. 4, pp. 2960–2974, 2015.

[2] A. R. Chiriyath, B. Paul, G. M. Jacyna, and D. W. Bliss, "Inner bounds on performance of radar and communications coexistence," *IEEE Transactions on Aerospace and Electronic Systems*, vol. 46, pp. 1185–1200, 2010.

[3] Y. Yao, J. Zhao, and L. Wu, "Adaptive waveform design for MIMO radar-communication transceiver," *Sensors*, vol. 18, no. 6, p. 1957, 2018.

[4] A. Hassanien, M. G. Amin, Y. D. Zhang, and F. Ahmad, "Phase-modulation based dual-function radar-communications," *IET Radar, Sonar & Navigation*, vol. 10, no. 8, pp. 1411–1421, 2016.

[5] Y. Yao and L. Wu, "Cognitive waveform design for radar-communication transceiver networks," *Journal of Advanced Transportation*, vol. 2018, pp. 1–11, 2018.

[6] A. Ahmed, Y. D. Zhang, and Y. Gu, "Dual-function radar-communications using QAM-based sidelobe modulation," *Digital Signal Processing*, vol. 82, pp. 166–174, 2018.

[7] D. W. Bliss, "Cooperative radar and communications signaling: the estimation and information theory odd couple," in *Proceedings of the IEEE Radar Conference*, pp. 50–55, Cincinnati, OH, USA, May 2014.

[8] Z. Geng, H. Deng, and B. Himed, "Adaptive radar beamforming for interference mitigation in radar-wireless spectrum sharing," *IEEE Signal Processing Letters*, vol. 22, no. 4, pp. 484–488, 2015.

[9] Z. Junhui, Y. Tao, G. Yi, W. Jiao, and F. Lei, "Power control algorithm of cognitive radio based on non-cooperative game theory," *China Communications*, vol. 10, no. 11, pp. 143–154, 2013.

[10] A. Khawar, A. Abdelhadi, and C. Clancy, "Target detection performance of spectrum sharing MIMO radars," *IEEE Sensors Journal*, vol. 15, no. 9, pp. 4928–4940, 2015.

[11] A. Ahmed, Y. D. Zhang, and B. Himed, "Distributed dual-function radar-communication MIMO system with optimized resource allocation," in *Proceedings of the IEEE Radar Conference*, Boston, MA, USA, April 2019.

[12] A. Hassanien, M. G. Amin, Y. D. Zhang, and F. Ahmad, "Dual-function radar-communications: information embedding using sidelobe control and waveform diversity," *IEEE Transactions on Signal Processing*, vol. 64, no. 8, pp. 2168–2181, 2016.

[13] A. Hassanien, M. G. Amin, Y. D. Zhang, and F. Ahmad, "Signaling strategies for dual-function radar communications: an overview," *IEEE Aerospace and Electronic Systems Magazine*, vol. 31, no. 10, pp. 36–45, 2016.

[14] X. Wang, A. Hassanien, and M. G. Amin, "Dual-function MIMO radar communications system design via sparse array optimization," *IEEE Transactions on Aerospace and Electronic Systems*, vol. 55, no. 3, pp. 1213–1226, 2019.

[15] A. Hassanien, B. Himed, and B. D. Rigling, "A dual-function MIMO radar-communications system using frequency-hopping waveforms," in *Proceedings of the 2017 IEEE Radar Conference (RadarConf)*, pp. 1721–1725, Philadelphia, PA, USA, May, 2017.

[16] D. DeLong Jr. and E. Hofstetter, "The design of clutter-resistant radar waveforms with limited dynamic range," *IEEE Transactions on Information Theory*, vol. 15, no. 3, pp. 376–385, 1969.

[17] A. Aubry, A. DeMaio, A. Farina, and M. Wicks, "Knowledge-aided (potentially cognitive) transmit signal and receive filter design in signal-dependent clutter," *IEEE Transactions on Aerospace and Electronic Systems*, vol. 49, no. 1, pp. 93–117, 2013.

[18] P. Stoica, H. He, and J. Li, "Optimization of the receive filter and transmit sequence for active sensing," *IEEE Transactions on Signal Processing*, vol. 60, no. 4, pp. 1730–1740, 2011.

[19] S. Kay, "Optimal signal design for detection of Gaussian point targets in stationary Gaussian clutter/reverberation," *IEEE Journal of Selected Topics in Signal Processing*, vol. 1, no. 1, pp. 31–41, 2007.

[20] M. Soltanalian, B. Tang, J. Li, and P. Stoica, "Joint design of the receive filter and transmit sequence for active sensing," *IEEE Signal Processing Letters*, vol. 20, no. 5, pp. 423–426, 2013.

[21] A. Aubry, M. Piezzo, A. De Maio, A. Farina, and M. Wicks, "Cognitive design of the receive filter and transmitted phase code in reverberating environment," *IET Radar, Sonar & Navigation*, vol. 6, no. 9, pp. 822–833, 2012.

[22] X. Song, P. Willett, S. Zhou, and P. B. Luh, "The MIMO radar and jammer games," *IEEE Transactions on Signal Processing*, vol. 60, no. 2, pp. 687–699, 2012.

[23] F. Gini, A. DeMaio, and L. Patton, *Waveform Design and Diversity for Advanced Radar Systems*, Institution of Engineering and Technology, London, UK, 2012.

[24] A. De Maio, Y. Yongwei Huang, and M. Piezzo, "A Doppler robust max-min approach to radar code design," *IEEE Transactions on Signal Processing*, vol. 58, no. 9, pp. 4943–4947, 2010.

[25] A. Aubry, A. De Maio, M. Piezzo, and A. Farina, "Radar waveform design in a spectrally crowded environment via nonconvex quadratic optimization," *IEEE Transactions on Aerospace and Electronic Systems*, vol. 50, no. 2, pp. 1138–1152, 2014.

[26] A. De Maio, Y. Huang, M. Piezzo, S. Zhang, and A. Farina, "Design of optimized radar codes with a peak to average power ratio constraint," *IEEE Transactions on Signal Processing*, vol. 59, no. 6, pp. 2683–2697, 2011.

[27] M. Ackroyd and F. Ghani, "Optimum mismatched filters for sidelobe suppression," *IEEE Transactions on Aerospace and Electronic Systems*, vol. AES-9, no. 2, pp. 214–218, 1973.

[28] R. Sato and M. Shinriki, "Simple mismatched filter for binary pulse compression code with small PSL and small S/N loss," *IEEE Transactions on Aerospace and Electronic Systems*, vol. 39, no. 2, pp. 711–718, 2003.

[29] J. Li, J. R. Guerci, and L. Xu, "Signal waveform's optimal-under-restriction design for active sensing," *IEEE Signal Processing Letters*, vol. 13, no. 9, pp. 565–568, 2006.

[30] A. De Maio, S. De Nicola, Y. Yongwei Huang, Z. Q. Zhi-Quan Luo, and S. Shuzhong Zhang, "Design of phase codes for radar performance optimization with a similarity constraint," *IEEE Transactions on Signal Processing*, vol. 57, no. 2, pp. 610–621, 2009.

[31] Y. Yao, J. Zhao, and L. Wu, "Frequency-hopping code design for target detection via optimization theory," *Journal of Optimization Theory and Applications*, vol. 10, pp. 1–26, 2019.

[32] M. Bica and V. Koivunen, "Generalized multicarrier radar: models and performance," *IEEE Transactions on Signal Processing*, vol. 64, no. 17, pp. 4389–4402, 2016.

[33] P. Stoica, J. Li, and M. Xue, "On binary probing signals and instrumental variables receivers for radar," *IEEE Transactions on Information Theory*, vol. 54, no. 8, pp. 3820–3825, 2008.

[34] P. Stoica, J. Li, and M. Xue, "Transmit codes and receive filters for radar," *IEEE Signal Processing Magazine*, vol. 25, no. 6, pp. 94–109, 2008.

[35] P. Stoica, M. Viberg, and B. Ottersten, "Instrumental variable approach to array processing in spatially correlated noise fields," *IEEE Transactions on Signal Processing*, vol. 42, no. 1, pp. 121–133, 1994.

[36] P. Stoica, J. Li, and M. Xue, "Transmit codes and receive filters for pulse compression radar systems," *IEEE Signal Processing Magazine*, vol. 10, pp. 3649–3652, 2008.

[37] J. Zhao, Q. Li, Y. Gong, and K. Zhang, "Computation offloading and resource allocation for cloud assisted mobile edge computing in vehicular networks," *IEEE Transactions on Vehicular Technology*, vol. 68, no. 8, pp. 7944–7956, 2019.

[38] A. Augusto, A. De Maio, and M. M. Naghsh, "Optimizing radar waveform and Doppler filter bank via generalized fractional programming," *IEEE Journal of Selected Topics in Signal Processing*, vol. 9, no. 8, pp. 1387–1399, 2015.

[39] M. M. Naghsh, M. Soltanalian, P. Stoica, M. Modarres-Hashemi, A. De Maio, and A. Aubry, "A Doppler robust design of transmit sequence and receive filter in the presence of signal-dependent interference," *IEEE Transactions on Signal Processing*, vol. 62, no. 4, pp. 772–785, 2014.

[40] A. Nemirovski, "Lectures on modern convex optimization," 2009, http://www.isye.gatech.edu/faculty-staff/profile.php?entry=an63.

[41] A. De Maio, Y. Huang, D. P. Palomar, S. Zhang, and A. Farina, "Fractional QCQP with applications in ML steering direction estimation for radar detection," *IEEE Transactions on Signal Processing*, vol. 59, no. 1, pp. 172–185, 2011.

[42] J. F. Sturm, "Using SeDuMi 1.02, a MATLAB toolbox for optimization over symmetric cones," *Optimization Methods and Software*, vol. 11, no. 1–4, pp. 625–653, 1999.

[43] Y. Chen, Y. Nijsure, C. Yuen, Y. H. Chew, Z. Ding, and S. Boussakta, "Adaptive distributed MIMO radar waveform optimization based on mutual information," *IEEE Transactions on Aerospace and Electronic Systems*, vol. 49, no. 2, pp. 1374–1385, 2013.

[44] S. Ni, J. Zhao, and Y. Gong, "Optimal pilot design in massive MIMO systems based on channel estimation," *IET Communications*, vol. 11, no. 7, pp. 975–984, 2016.